0026-895X/06/7005-1565–1574$20.00
MOLECULAR PHARMACOLOGY
Copyright © 2006 The American Society for Pharmacology and Experimental Therapeutics
Mol Pharmacol 70:1565–1574, 2006

Vol. 70, No. 5
28647/3147427
Printed in U.S.A.

Transmembrane Domain VII of the Human Apical Sodium-Dependent Bile Acid Transporter ASBT (SLC10A2) Lines the Substrate Translocation Pathway

Naissan Hussainzada, Antara Banerjee,[1] and Peter W. Swaan

Department of Pharmaceutical Sciences, University of Maryland, Baltimore, Maryland.

Received July 7, 2006; accepted August 9, 2006

ABSTRACT

Recent evidence implicating transmembrane (TM) segment 7 of the apical sodium-dependent bile acid transporter (ASBT) in substrate interaction warranted examination of its aqueous accessibility. Therefore, cysteine substitution of 22 consecutive amino acids was performed against a methanethiosulfonate (MTS)-resistant background (C270A). Activity and susceptibility to polar MTS derivatives [(2-aminoethyl)-methanethiosulfonate (MTSEA), [2-(trimethylammonium)ethyl]methanethiosulfonate (MTSET), and methanethiosulfonate ethylsulfonate (MTSES)] of mutants were evaluated in COS-1 cells. Thr289, Tyr293, Gln297, Ala301, Phe307, and Tyr308 represented loss-of-function mutants; furthermore, the measurable residual activities for T289C, Y293C, and A301C (≤20% control) proved insensitive to MTS treatment. MTSES and MTSET inhibition was confined to residues lining the extracellular half of TM7; amino acids situated deeper within the membrane were unaffected. In contrast, the entire length of TM7 was susceptible to the relatively smaller MTSEA; moreover, MTSEA sensitivity was significantly amended by coapplication with substrates. This selective pattern of modification suggests that the highly conserved lower half of TM7 lies within a water-filled cavity easily accessible from the extracellular milieu, whereas residues approaching the cytosolic/membrane interface reside in pores for which accessibility is modulated by molecular volume. Functionally inactive and MTS-inaccessible residues (T289C, Y293C, Q297C, and A301C) within TM7 may play a structural role critical to transporter function; conversely, MTS-sensitive residues are spatially distinct and may demarcate a face of the TM involved in substrate translocation. In addition, computational analysis of solvent-accessible domains identified five key solvent pockets that predominantly line the hydrophilic face of TM7. Combined, our data suggest that TM7 plays a dominant role in the hASBT translocation process.

Bile acid transporters belong to the solute carrier 10 (SLC10) family of integral membrane proteins (Geyer et al., 2006), comprising the Na^+-taurocholate cotransporting polypeptide (Ntcp, SLC10A1) expressed in the liver, the apical sodium-dependent bile acid transporter (ASBT, SLC10A2) expressed primarily in the intestine and cholangiocytes, three still-uncharacterized but homologous transporter proteins (SLC10A3–5), and a recently identified sodium-dependent organic anion transporter (SOAT, SLC10A6) that is intriguingly homologous to ASBT but does not seem to transport bile acids (Geyer et al., 2004). Together, ASBT and the Na^+-taurocholate cotransporting polypeptide effectively maintain the enterohepatic recycling of bile acids within the gastrointestinal tract and the liver, respectively. Through sensing and modulation of the bile acid receptor, a reduction of the human bile acid pool leads to de novo synthesis of bile salts from plasma cholesterol mediated by hepatic CYP7A. Thus, bile acid transporters play a critical role in cholesterol homeostasis (Chiang et al., 2001; Trauner and Boyer, 2003), and ASBT in particular has emerged as a valuable pharmacological target for cholesterol lowering therapy (Izzat et al., 2000; Huff et al., 2002; Li et al., 2004; Alrefai et al., 2005), soliciting the design of specific ASBT inhibitors (Root et al., 1995; Kramer et al., 1999; West et al., 2002; Telford et al., 2003). Despite its clinical significance, very little is known concerning the structural aspects of ASBT and how they relate to its function and ligand recognition. We have re-

This research was supported by grant DK061425 (to P.W.S.) from the National Institutes of Health, National Institute for Digestive Diseases and Kidney.

A.B. and N.H. contributed equally to this work.

[1] Current affiliation: Schering-Plough Biopharma, Palo Alto, California.

Article, publication date, and citation information can be found at http://molpharm.aspetjournals.org.
doi:10.1124/mol.106.028647.

ABBREVIATIONS: SLC10, solute carrier 10; ASBT, apical sodium-dependent bile acid transporter; hASBT, human apical sodium-dependent bile acid transporter; TM, transmembrane; SCAM, substituted cysteine accessibility method; TCA, taurocholic acid; GDCA, glychodeoxycholic acid; CA, cholic acid; sulfo-NHS-SS-biotin, (sulfosuccinimidyl 2-(biotinamido)-ethyl-1,3-dithiopropionate; MTSEA-biotin, *N*-biotinaminoethyl methanethiosulfonate; *wt*, wild type; PBS, phosphate-buffered saline.

cently shown that hASBT is composed of seven transmembrane-spanning segments (Banerjee and Swaan, 2006), with a cytosolic carboxyl terminus and an extracellular amino terminus bearing an *N*-linked glycosylation site (Zhang et al., 2004).

Residues within transmembrane (TM) domains of transporter proteins often play an intricate role in substrate translocation. In general, the functional importance and aqueous accessibility of amino acid residues in these TM regions can be tested by the substituted cysteine accessibility method (SCAM). In this approach, consecutive residues of a putative TM domain are replaced by cysteine. The sulfhydryl group of the introduced cysteine is likely to be protonated if the residue faces a water-accessible translocation pathway. As the thiolate moiety reacts 10^9 times faster with polar MTS reagents compared with free sulfhydryl, the resulting reaction provides excellent selectivity (Akabas et al., 1992). Thus, the alkylation of an engineered cysteine in the translocation pathway should affect binding or transport irreversibly and should be reduced by the presence of a competitive ligand or inhibitor.

So far, there has been no systematic analysis of the functional role of TM regions in hASBT. The studies presented here sought to examine TM7, which serves as an attractive target for a variety of reasons: 1) there is a high degree of sequence identity and homology (>90%) within TM7 among a large number of species, ranging from fish to humans (Fig. 1B); 2) photoaffinity labeling studies of the rat ileum (Kramer et al., 2001) have previously identified a ~7-kDa region corresponding to this domain as a potential site for bile acid interaction; 3) residues Ser294 and Ile295 of human ASBT (corresponding to Thr294 and Val295 in mouse; Fig. 1B) were identified as singularly responsible for the almost 150-fold shift in affinity seen in humans versus mice for 2164U90, a benzothiazepine-based competitive inhibitor (Hallén et al., 2002); and 4) one of the main phenotypes for primary bile acid malabsorption syndrome has been attributed to a single nucleotide transition (C to T) resulting in a Pro to Ser substitution at amino acid position 290 (P290S) within TM7, leading to a dysfunctional mutant (Wong et al., 1995). Thus, TM7 has been strongly implicated in hASBT function and therefore constitutes an appealing target for SCAM that may offer valuable insights into the structure-function relationship of a highly conserved TM region.

The SCAM technique mostly necessitates the use of a functional Cys-less mutant or a protein whose native cysteine residues are unreactive toward thiol modifiers (Chen et al., 1997; Kulkarni et al., 2003a,b). Our group and others have shown previously that a Cys-less mutant hASBT is not functional and that MTS reagents significantly decrease uptake activity of native hASBT (Hallén et al., 2000; Banerjee et al., 2005), thus rendering it an inappropriate scaffold for SCAM studies. However, subsequent mutagenesis analysis of native hASBT cysteines showed that a C270A hASBT mutant retains full transport activity and remains largely unaffected in the presence of thiol modifiers (Banerjee et al., 2005). To help define the transport pathway for bile acids, we have used this mutant as a background for the cysteine substitution of 22 consecutive residues in TM7 to test their sensitivity to MTS reagents.

Experimental Procedures

Materials. [^{3}H]Taurocholic acid (0.2 Ci/mmol) was purchased from American Radiolabeled Chemicals, Inc. (St. Louis, MO); taurocholic acid (TCA), glychodeoxycholic acid (GDCA), and cholic acid (CA) were purchased from Sigma (St. Louis, MO); (sulfosuccinimidyl 2-(biotinamido)-ethyl-1,3-dithiopropionate (sulfo-NHS-SS-biotin) from Pierce Chemical Co. (Rockford, IL); *N*-biotinaminoethyl methanethiosulfonate (MTSEA-biotin) and MTS reagents: (2-aminoethyl)-methanethiosulfonate (MTSEA), [2-(trimethylammonium) ethyl] methanethiosulfonate (MTSET), and methanethiosulfonate ethyl-

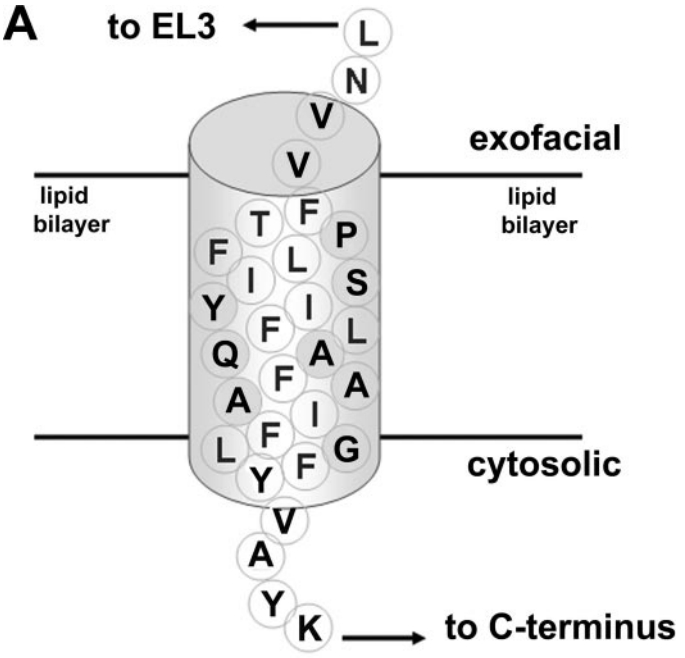

Fig. 1. One-letter amino acid designation and sequence homology of residues spanning TM7 of hASBT. A, a secondary structure model of TM7 highlighting its putative arrangement within the plasma membrane and the identity of the 22 amino acid residues individually mutated to cysteine, from Phe287 to Tyr308. Residues preceding Phe287 lead into extracellular loop 3 that connects TM6 and TM7, whereas residues after Tyr308 mark the beginning of the C-terminal tail of hASBT. B, multiple sequence alignment of TM7 residues mutated in this study among diverse range of species expressing ASBT (SLC10A2) retrieved from GeneBank in FASTA format and aligned via ClustalW routine. Annotation was performed with the MPSA program. Amino acid homology is noted as follows: *, fully conserved; :, high consensus; ·, low consensus. The numbers designate the amino acid position within the sequence of ASBT and the bottom line of amino acids represents the primary consensus.

sulfonate (MTSES) from Toronto Research Chemicals, Inc., (North York, ON, Canada). Cell culture media and supplies were obtained from Invitrogen (Carlsbad, CA). All other reagents and chemicals were of highest purity available commercially.

Cell Culture and Transient Transfections. COS-1 cells (American Type Culture Collection, Manassas, VA) were maintained in Dulbecco's modified Eagle's medium containing 10% fetal calf serum, 4.5 g/liter glucose, 100 units/ml penicillin, and 100 μg/ml streptomycin (Invitrogen) at 37°C in a humidified atmosphere with 5% CO_2. Transient transfection of *wt*, C270A and cysteine mutants into COS-1 cells were performed as described previously (Banerjee et al., 2005).

Site-Directed Mutagenesis. Because mutation of key native cysteines within hASBT produces an inactive protein, the constructed mutant C270A was used as the template for further incorporation of individual cysteine mutations into TM7. The C270A mutant has been shown previously to retain function at levels comparable with native protein and proves resistant to thiol modification (Banerjee et al., 2005) (Fig. 1B). Site-directed mutations were introduced using the QuikChange site-directed mutagenesis kit from Stratagene (La Jolla, CA) according to the manufacturer's instructions. The pCMV5 vector containing human ASBT cDNA (a kind gift of Dr. Paul Dawson, Wake Forest University, Winston-Salem, NC) was used as the template in subsequent polymerase chain reaction mutagenesis reactions to generate the C270A construct. Mutagenesis primers used to integrate the site-directed amino acid substitutions into the C270A template were custom-synthesized and purchased from Sigma-Genosys (The Woodlands, TX). Plasmid purification was accomplished using a kit from Roche (Indianapolis, IN) with verification of amino acid replacement for all mutants performed by DNA sequencing using a 3700 DNA analyzer (Applied Biosystems, Foster City, CA) at the Plant-Microbe Genomics Facility of the Ohio State University.

Uptake Assay, Western Blot Analysis, and Cell Surface Biotinylation. Initial rates of ligand uptake were determined by incubation of transfected COS-1 cells in modified Hanks' balanced salt solution (MHBSS), pH 7.4, uptake buffer containing 5.0 μM [^{3}H]TCA at 37°C for 12 min. We have found previously (Banerjee et al., 2005; Banerjee and Swaan, 2006) that this uptake period ensures linear steady-state kinetics in conjunction with an optimal signal-to-noise ratio for subsequent [^{3}H]TCA analysis via liquid scintillation counting. Uptake was halted by a series of washes with ice-cold Dulbecco's PBS, pH 7.4, containing 0.2% fatty acid free bovine serum albumin and 0.5 mM TCA. Cells were lysed in 350 μl of 1 N NaOH and subjected to liquid scintillation counting using an LS6500 liquid scintillation counter (Beckman Coulter, Inc., Fullerton, CA) and total protein quantification using the Bradford protein assay (Bio-Rad Laboratories, Hercules, CA). Uptake activity was calculated as picomoles of [^{3}H]TCA internalized per minute per milligram of protein.

For immunoblotting studies, transfected COS-1 cells were washed in PBS and lysed in 0.2 ml of lysis buffer B (25 mM Tris, pH 7.4, 300 mM NaCl, 1 mM $CaCl_2$, 1% Triton X-100, and 0.5% Sigma protease inhibitor cocktail), separated on a 12.5% SDS-polyacrylamide gel, and transferred onto an Immunoblot polyvinylidene difluoride membrane (Bio-Rad). Blots were probed with rabbit anti-ASBT 1° antibody (1:1000) and visualized using goat anti-rabbit IgG/HRP conjugated 2° antibody with chemiluminescent detection (ECL Plus Western Blot kit; GE Healthcare, Little Chalfont, Buckinghamshire, UK). For cell surface biotinylation, transfected COS-1 cells were incubated with either sulfo-NHS-SS-biotin or MTSEA-biotin for 30 min at RT (Wong et al., 1995; Mitchell et al., 2004). After several washes with PBS containing 1.0 mM $CaCl_2$ and $MgCl_2$, cells were disrupted with lysis buffer B at 4°C for 20 min (Zhang et al., 2004). After centrifugation, biotinylated proteins were recovered overnight at 4°C using 100 μl of streptavidin agarose beads. Samples were eluted with SDS-polyacrylamide gel electrophoresis buffer, and immunoblotting was carried out as described above. Blots were also probed for the presence of α-integrin, a 150-kDa plasma membrane protein, and the absence of calnexin, a 90-kDa endoplasmic reticulum protein, which represent positive and negative controls, respectively, to assess the integrity of the biotinylation procedure (calnexin data not shown).

MTS Inhibition Studies. Sensitivity to hydrophilic, charged MTS reagents was assessed by pretreatment of transiently transfected COS-1 cells with either 1 mM MTSES, 1 mM MTSET, or 2.5 mM MTSEA for 10 min at room temperature. After MTS treatment, cells were washed twice in modified Hank's balanced salt solution (Sigma), and [^{3}H]TCA uptake was measured as described above. Because of the short half-lives of MTS compounds in aqueous buffer, all reagents were freshly prepared before each study.

Substrate Protection Assays. To determine whether the presence of substrate can protect against MTSEA labeling, transfected COS-1 cells were washed twice in 1× PBS, pH 7.4, followed by coincubation with 2.5 mM MTSEA and either GDCA or CA (200 μM) for 10 min at room temperature. Thereafter, cells were washed twice in MHBSS, pH 7.4 and additionally equilibrated for 15 min at 37°C and [^{3}H]TCA uptake was determined as described above. All control wells were treated identically.

Sodium Activation. To assess the importance of extracellular [Na^+] in transport function of cysteine mutants, [^{3}H]TCA uptake was measured at low (12 mM) sodium concentrations (uptake conducted as described above), using choline chloride as an equimolar replacement for NaCl. A ratio of TCA uptake at 12 versus 137 mM [Na^+] was calculated for each mutant. Thus, ratios of 1 signify no measurable effect of extracellular [Na^+] on transport activity for cysteine mutants, whereas fractions less than 1 imply greater necessity for physiological [Na^+] to ensure proper function.

Computational Analysis. Helical wheel representations of TM7 were generated using the Lasergene software 6.0 (DNAstar, Madison, WI). Analysis of residue placement and solvent accessibility within hASBT and surrounding TM7 was assessed using a previously developed three-dimensional model for hASBT (Zhang et al., 2004) The SiteID subroutine within the SYBYL software suite (version 6.9; Tripos Associates, St. Louis, MO) was employed to determine binding pockets. SiteID uses an atom-based solvent accessibility method for the detection of local clefts. The Grid algorithm was used to detect deep pockets and tight cavities within the protein. The grid was specified using a 1.0-Å resolution and 3.0-Å protein film depth. All other parameters were set to default values, except for the minimum population of grid points in a cluster, which was set to 15. Solvent was allowed to access the protein inner core from both the extracellular and intracellular environment. Thus, the results represent *overall* solvent accessibility. Images were rendered within the Biopolymer module of SYBYL and transferred to Adobe Photoshop CS (ver. 9.0; Adobe Systems, Mountain View, CA) for annotation.

Data Analysis. For each mutant, data are represented as mean ± S.D. of at least three different experiments with triplicate measurements. Data analysis was performed with Prism 4.0 (GraphPad Software, San Diego, CA) using analysis of variance with Dunnett's post hoc test. Data were considered statistically significant at $p \leq 0.05$.

Results

Cysteine Scan of Transmembrane Domain 7. Figure 1 illustrates the identity and sequence alignment of amino acids 287 to 308 of the human ASBT. This region is predicted to form TM7 and is highly conserved among a range of evolutionarily diverse species, particularly along the extracellular half of the helix, between amino acids Phe287 and Gln297. In this study, each amino acid within TM7 was mutated to a cysteine residue, resulting in 22 individual mutant transporters (Table 1). The parental scaffold for these mutations was a hASBT mutant designated C270A,

which contains an alanine substitution at one of the 13 endogenous cysteines present in the native transporter. C270A displays activity comparable with *wt*-ASBT (Fig. 2) but, unlike the native transporter, proves insensitive to all polar MTS reagents at the maximal concentrations used in this study (2.5 mM). These results suggest either that 1) MTS accessibility of endogenous cysteines within hASBT is limited to Cys270 or 2) MTS labeling of cysteines other than Cys270 is functionally silent. Employing amino acid-specific surface labeling, we observed considerable differences in tagging of C270A by the membrane impermeant biotinylation reagent sulfo-NHS-SS-biotin, reactive only with lysines and MTSEA-biotin, which exclusively targets cysteines; in contrast, *wt*-ASBT levels remained relatively unaffected (Fig. 2C). Some residual MTSEA-biotin labeling of C270A remains; however, it is a very small fraction of the bands obtained with *wt* samples. Thus, the vast majority of MTS susceptibility within the native protein, at least from the extracellular milieu, is conferred by the cysteine at the 270 position; however, this sensitivity can be ameliorated by conversion to alanine, qualifying the C270A mutant as a suitable parental template for SCAM.

Transport Activity and Membrane Expression of Cysteine-Substituted Mutants. All constructed cysteine mutants were transiently transfected into the monkey kidney fibroblast cell line COS-1 and screened for transport activity (Fig. 3A). Cell surface expression of mutants was measured using biotin labeling and immunoblotting (Fig. 3B) supplemented with densitometric analysis of developed bands (Fig. 3C). Most mutant transporters exhibited substantial transport activity (Fig. 3) compared with C270A control, which exhibited a [^{3}H]TCA uptake activity of 104.99 ± 13.83 pmol/min/mg of protein. Two mutants (F287C and L291C) retained between 55 to 60% activity of the parental (C270A) transporter; however, a total of six mutants were either completely inactive (Q297C, F307C, and Y308C) or had less than 20% activity (F289C, Y293C, and A301C), which was not correlated to their cell surface expression. However, the remaining functional activities of both A301C and Y308C were decreased together with a significant reduction in their cell surface expression (Fig. 3D), suggesting impairments in trafficking and insertion into the plasma membrane for these mutations; conversely, mutant F307C

TABLE 1

Cysteine scanning mutagenesis of transmembrane domain 7

hASBT cDNA encoding the C270A mutation were used as the template to generate each of the 22 cysteine double mutants (i.e. Cys270Ala/Phe287Cys using oligonucleotide site-directed mutagenesis). C270A proves resistant to MTS modification and was hence used as the template for all mutations.

No.	Amino Acid Mutation[a]	Codon Change
1	Phe287Cys	TTC→TGC
2	Thr288Cys	ACC→TGC
3	Phe289Cys	TTC→TGC
4	Pro290Cys	CCG→TGC
5	Leu291Cys	CTC→TGC
6	Ile292Cys	ATC→TGC
7	Tyr293Cys	TAC→TGC
8	Ser294Cys	AGC→TGC
9	Ile295Cys	ATT→TGT
10	Phe296Cys	TTC→TGC
11	Glu297Cys	CAG→TGC
12	Leu298Cys	CTC→TGC
13	Ala299Cys	GCC→TGC
14	Phe300Cys	TTT→TGT
15	Ala301Cys	GCC→TGC
16	Ala302Cys	GCA→TGT
17	Ile303Cys	ATA→TGT
18	Phe304Cys	TTC→TGC
19	Leu305Cys	TTA→TGT
20	Gly306Cys	GGA→TGT
21	Phe307Cys	TTT→TGT
22	Tyr308Cys	TAT→TGT

[a] Represents the position of the mutation of a particular amino acid to a cysteine.

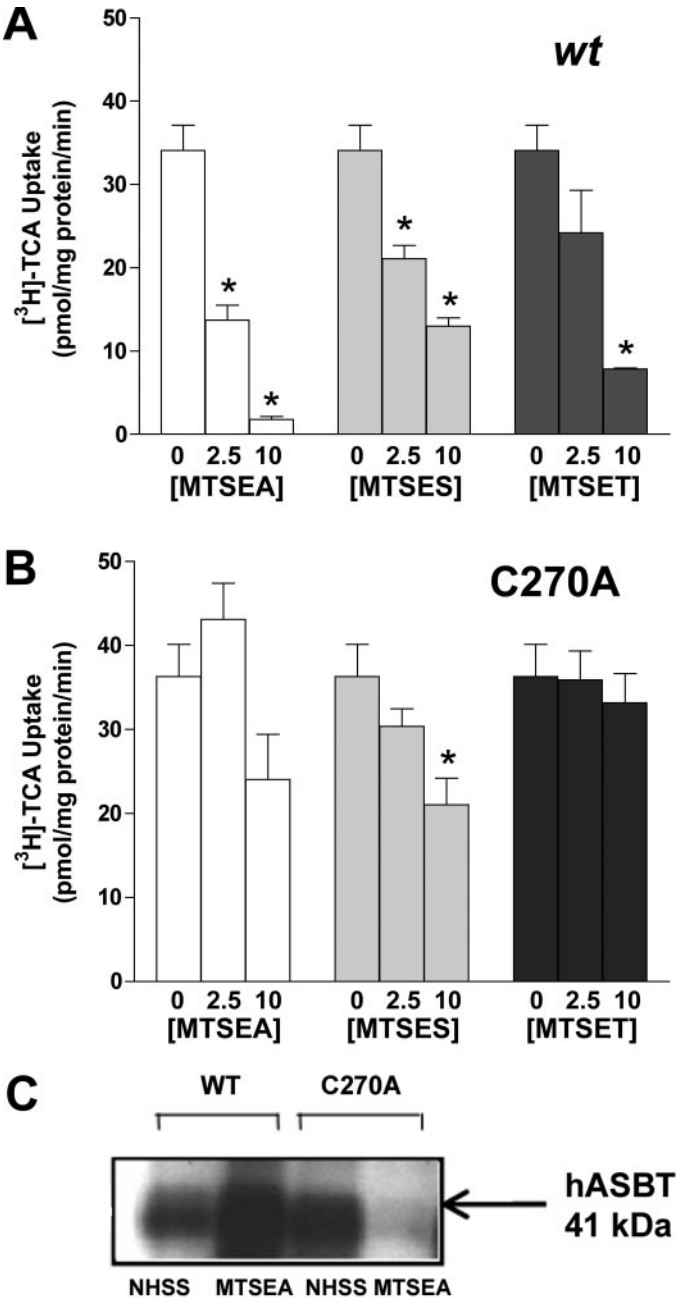

Fig. 2. MTS sensitivity and cysteine accessibility of *wt* and C270A. A and B, COS-1 cells transfected with *wt* and C270A were pretreated with varying concentrations of MTSEA (white bars), MTSES (gray bars), and MTSET (dark gray bars) for 10 min at room temperature. Preincubation solutions were washed away and followed by measurement of [^{3}H]TCA uptake activity for 12 min at 37°C. C, intact COS-1 cells transfected with *wt* and C270A were labeled with sulfo-NHS-SS biotin and MTSEA-biotin as described under *Experimental Procedures* and processed for Western blot analysis. Blots were probed with anti-hASBT antibodies (1:1000 dilution) followed by horseradish-peroxidase-linked anti-rabbit immunoglobulin at a dilution of (1:30,000). The 41-kDa bands depict the glycosylated forms of hASBT for *wt* and C270A.

lacked expression either at the plasma membrane (Fig. 3B) or in whole-cell lysate preparations (data not shown), suggesting that mutation at this position altered proper folding or synthesis of the protein. Therefore, the severe loss of activity for Y308C (<5% activity of C270A parent) coupled with its exceedingly low membrane expression (25% of C270A parent) suggests a structural role for this amino acid also. It is noteworthy that a number of mutants exhibited appreciable transport activity but greatly reduced membrane expression, including F296C, A302C, and G306C, suggesting that these mutations may have increased activity or decreased K_m. Because of their exceedingly low levels of measurable transport activity, mutants Q297C, F307C, and Y308C were omitted from future studies.

Sensitivity to MTS Reagents. Nineteen mutants with appreciable transport activity were examined for their sensitivity to 1 mM MTSES, 1 mM MTSET, and 2.5 mM MTSEA. These methanethiosulfonate derivatives react rapidly and selectively with the protonated sulfhydryl moieties of cysteine residues to create covalent attachment introducing either a positively charged ethylamine (MTSEA), a negatively charged ethylsulfonate (MTSES), or a bulkier ethyl trimethylammonium (MTSET) group (Akabas et al., 1992). Both MTSES and MTSET are membrane-impermeant, whereas MTSEA can permeate the membrane in its uncharged form (Akabas et al., 1992). Irrespective of their ability to traverse the plasma membrane, reaction of MTS reagents with cysteine can only appreciably occur when the

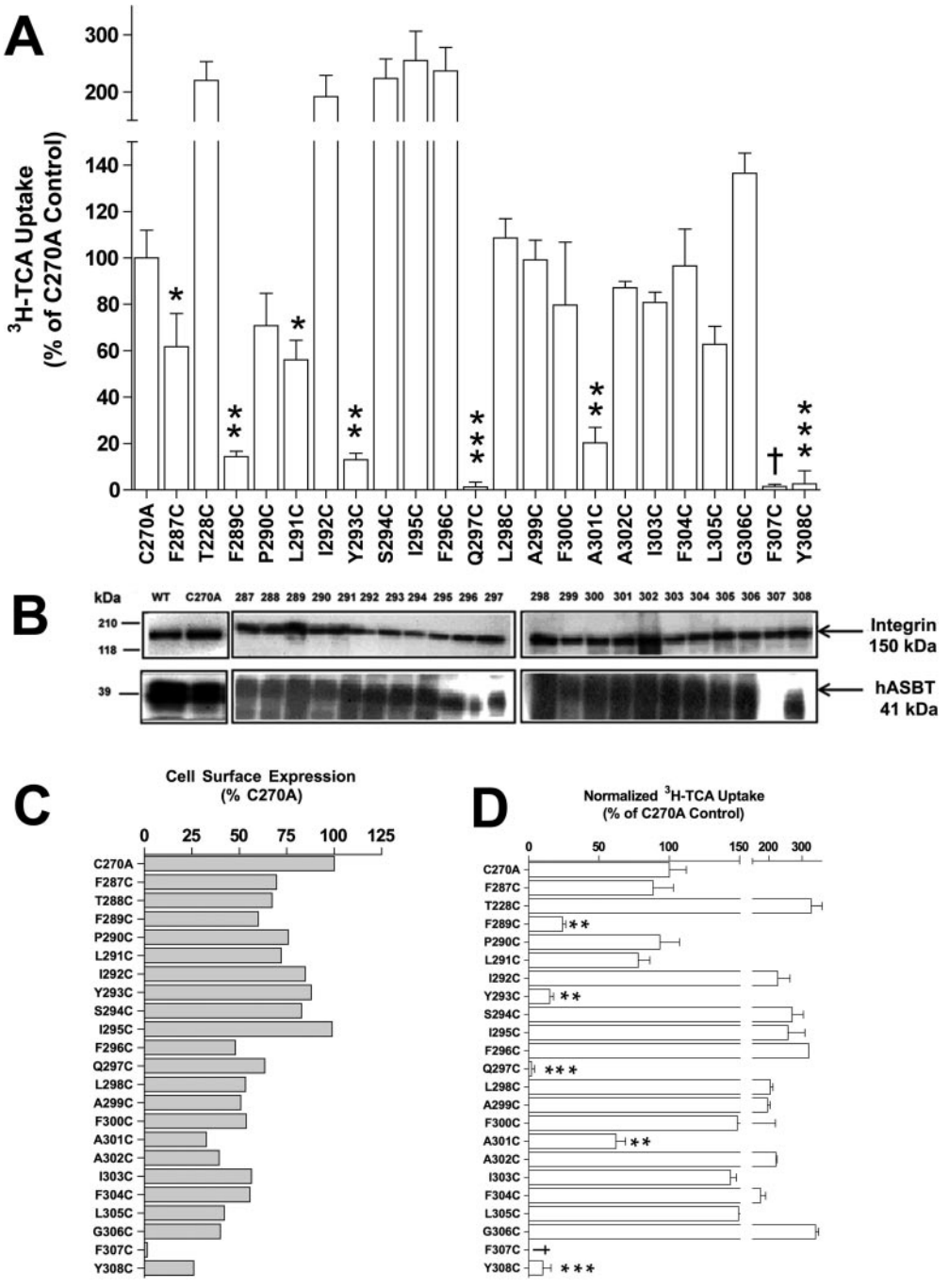

Fig. 3. Activity and expression of cysteine double mutants of hASBT expressed in COS-1 cells. A, COS-1 cells expressing TM7 cysteine-substituted double mutants were screened for initial [^{3}H]TCA uptake activity for 12 min at 37°C. Activity for each mutant was normalized to total protein content and expressed as a percentage of parental control (C270A). Background uptake activity for COS-1 cells transfected with plasmid vector only were subtracted from activity of each mutants. Data for each mutant is represented as mean ± S.D. of three separate experiments. ***, $p \leq 0.001$; **, $p \leq 0.01$; and *, $p \leq 0.05$. B, intact transfected COS-1 cells were treated with sulfo-NHS-SS-biotin as described under *Experimental Procedures* followed by Western blot processing. Bands were detected by immunoblotting with the anti-hASBT antibody as described under *Experimental Procedures*. Mature glycosylated hASBT is visualized as the band at 41 kDa, whereas the 38-kDa band (not indicated) represents the unglycosylated species. α-Integrin (150 kDa) was used as an internal plasma membrane marker for the biotinylated fractions; blots were also probed for the absence of calnexin (90 kDa) (data not shown), an endoplasmic reticulum marker protein acting as a negative control to ensure integrity of surface labeling. Marker lanes are shown on the left side of the individual blots. C, averaged densitometric analysis ($n = 2$) of the surface expression for control and cysteine mutants normalized to internal marker (α-integrin) and represented as a percentage of C270A parent. D, [^{3}H]TCA uptake activity after normalization for average cell surface expression.

sulfhydryl side group is solvent-accessible. This is because the ionized, or more reactive, sulfhydryl species is strongly disfavored by the low dielectric constant of the lipid environment; thus, it can be assumed that side-chain modification of the introduced cysteine residues occurs only in aqueous environments (Karlin and Akabas, 1998). In particular, we can posit that cysteine side chains reactive with MTSEA face either the extracellular or intracellular milieu or an aqueous intramembrane compartment. On the other hand, MTSES and MTSET-reactive side chains can face either the extracellular milieu or a water-filled intramembranous pore accessible only from the extracellular space (Javitch, 1998).

In the current study, the C270A parental template demonstrated insensitivity to all MTS reagents (Figs. 2 and 4) used. Despite exhibiting only ≤20% activity of C270A, mutant transporters F289C, Y293C, and A301C were assayed nonetheless for potential sensitivity to thiol modification. Absence of additional reduction in activity in the presence of all three MTS reagents suggested minimal water accessibility of these residues. In the interest of clarity of data interpretation, these data have been omitted.

For the remaining sixteen functionally active mutants, both MTSES and MTSET (Fig. 4, A and B) produced significant inhibition of activity (≤30% activity of C270A parent) almost exclusively for residues lining the extracellular half of the transmembrane domain (F287C, T288C, P290C, L291C, I292C, S294C, and L298C), which is coincidentally the region of the TM with the greatest sequence conservation (Fig. 1B). Only mutants I295C, F296C, and L305C were selectively inhibited by MTSES (≤25% activity of C270A parent) but not MTSET to a significant degree ($p \leq 0.01$). Although statistically insignificant, modest MTSES inhibition was consistently observed for a number of residues situated deeper into the lipid membrane approaching the cytosolic interface. Therefore, we may infer either that the introduced cysteines at these selectively modified positions simply may not be accessible to MTSET, or they are accessed and modified with minimal functional consequences. Although the latter explanation is possible, it is more likely that the disparity in molecular volumes between these two MTS derivatives (109 versus 90 Å^3) is responsible for constraining MTSET solvent accessibility along the cytosolic half of the TM, especially if these residues are partially buried or more deeply embedded within the lipid membrane. In summary, these data strongly suggest unrestricted accessibility along the extracellular half of TM7 that decreases as a function of increasing depth into the membrane and relative size of the probe.

In addition to MTSES and MTSET, the sensitivity of TMD7 cysteine mutants to the relatively smaller (69 Å^3) MTSEA was also examined (Fig. 4C). Application of 2.5 mM MTSEA produced an inhibition profile identical to MTSES along the extracellular, highly accessible half of the TM, although inhibition was slightly more severe (≤20% activity of C270A parent). However, toward the latter half of TM7 previously inhibited only partially by MTSES, highly significant ($p \leq 0.01$) MTSEA inhibition (ranging from 10–40% activity of C270A parent) was demonstrated for five residues (A299C, F300C, A302C, F304C, G306C). As previously noted, MTSEA may traverse the membrane to potentially access intramembraneous residues from the cytosol; however, this membrane permeability only occurs with the uncharged species. MTSEA exhibits a pk_a of approximately 8.5 (calculated using the SPARC system at http://ibmlc2.chem.uga.edu/sparc/); therefore, the prevalence of its uncharged species at

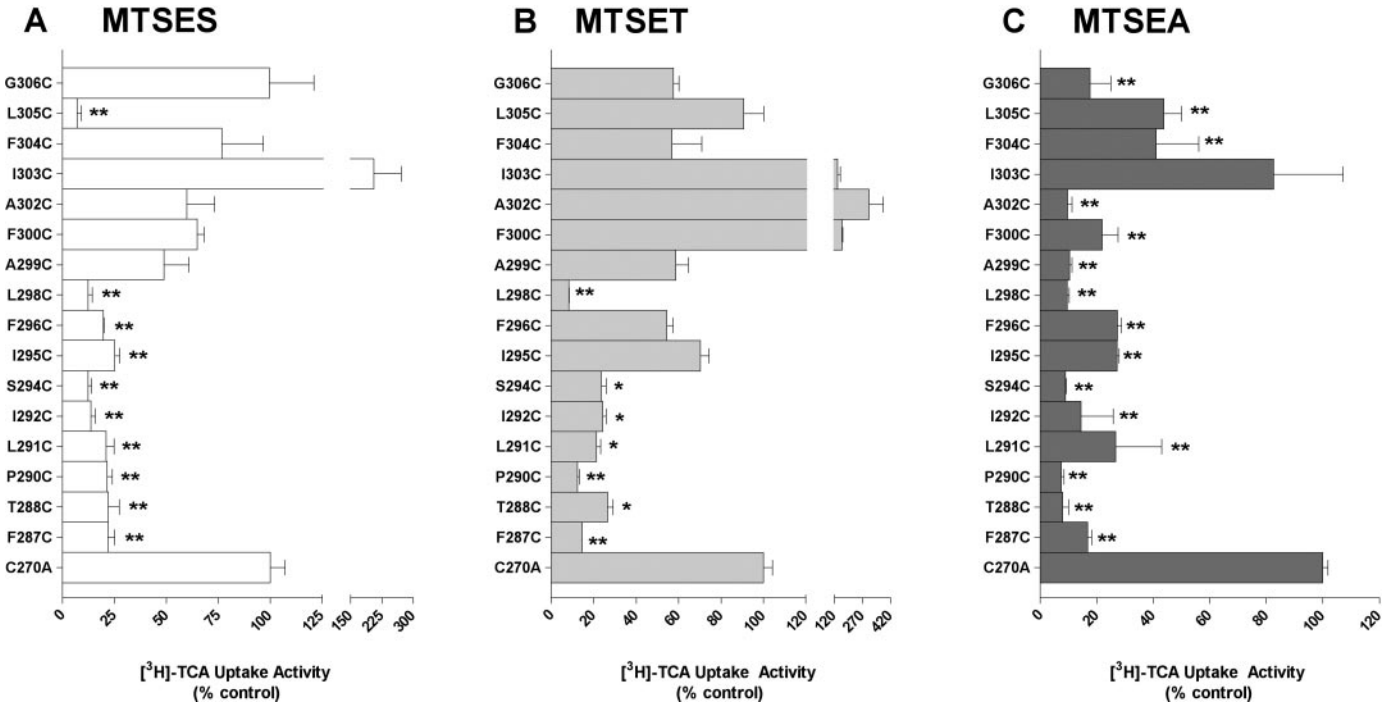

Fig. 4. Accessibility of TM7 cysteine double mutants to polar MTS reagents. Transfected COS-1 cells were incubated with 1.0 mM MTSES (A), 1 mM MTSET (B), and 2.5 mM MTSEA (C) for 10 min at room temperature. Functionally inactive mutants (Q297C, F307C, and Y308C) were excluded from this study. Preincubation solutions were washed away, and the remaining uptake activity of [^{3}H]TCA was measured. Uptake activities for each mutant pretreated with MTS reagents are normalized to respective uptakes in control wells and expressed as a percentage of C270A. Uptake activity of control (C270A) in the presence of MTSES, MTSET and MTSEA was 102.39 ± 10.49, 106.89 ± 6.01, and 88.17 ± 1.74 pmol/min/mg protein, respectively. The values represent the means ± S.D. (n = 2–3 separate experiments). ***, $p \leq 0.001$; **, $p \leq 0.01$; *, $p \leq 0.05$, compared with C270A.

physiological pH is calculated to be less than 8% of the applied concentration. Although the conditions of the current study (pH 7.4) preclude significant accumulation of the unprotonated species on the intracellular (*trans*) side, we cannot exclude the possibility that *trans* modification of intracellular cysteine residues may occur. However, the generally short half-life of MTSEA in aqueous buffer in combination with a 30-fold slower reaction rate for *trans* modification diminishes the likelihood of MTSEA modification from the intracellular domain (Holmgren et al., 1996). Thus, we may speculate that MTSEA readily accesses regions of the TM that are still solvent-accessible from the extracellular space; yet, MTSES and MTSET, because of their increased molecular volumes and decreased effective concentrations at the reaction site (1.0 versus 2.5 mM), may not sufficiently access these regions for extensive modification. Nonetheless, our results clearly demonstrate the high degree of water-accessibility of TM7, particularly at positions constituting its extracellular half, consistent with the conclusion that TM7 amino acids line a water-filled pore or cavity.

Effect of Substrates on MTSEA Sensitivity. To determine whether the presence of bile acid substrates ameliorates MTSEA-sensitivity of cysteine mutants, MTSEA preincubation was performed in the presence of GDCA or CA (200 μM). These bile acids display different substrate affinities for hASBT, with an approximately 16-fold decrease in K_m for GDCA (2.0 $\pm$ 0.4 μM) compared with CA (33.3 $\pm$ 12.8 μM) (Craddock et al., 1998). In theory, this difference in apparent affinities for these substrates should reflect correspondingly in their ability to shield susceptible mutants from MTSEA. Among the three MTS reagents investigated, MTSEA was chosen because of its more pronounced effect on the activities of the mutant transporters. For all MTSEA-sensitive mutants, coincubation with GDCA and CA resulted in transport activities at least 50% higher than activity observed in the presence of 2.5 mM MTSEA alone (Fig. 5). Thus, significant protective effects against thiol modification of TM7 mutants could be exerted by both bile acid substrates; however, no correlation between differing bile acid affinities and degree of conferred protection could be made. Complete restoration of activity was only observed for mutants I298C and I303C (Fig. 5). Several possible explanations may account for bile acid substrate protection from MTSEA modification. For example, substrate binding or translocation along these sites can physically prevent MTSEA access to the introduced cysteine. On the other hand, conformational changes occurring after binding of bile acid substrates could occlude or block the substituted cysteine, thereby hampering MTSEA labeling. Because this highly conserved, typically hydrophobic membrane region displays prominent water accessibility, it is dubious that this region would be functionally inert; therefore, we disfavor the conclusion that TM7 becomes inaccessible to MTSEA due only to conformational effects without any participation in substrate interaction events. Although some sites within TM7 may indeed become inaccessible because of downstream conformational changes after substrate binding and/or internalization, we hypothesize that substrate protection of TM7 probably occurs as a result of the presence of substrate within its highly water-accessible regions.

Sodium Dependence of TM7 Cysteine Mutants. Previous studies have shown that bile acid uptake via hASBT is electrogenic, with a Na^+/bile acid stoichiometry of 2:1 (Weinman et al., 1998). Therefore, the functional consequences of lowered [Na^+] were evaluated for 16 mutants with measurable transport. For each mutant transporter, [^{3}H]TCA internalization was measured at 12 mM and taken as a ratio of its corresponding uptake at 137 mM [Na^+]. Using this protocol, we can deduce any silent functional deficiencies resulting from cysteine substitution not apparent at physiological [Na^+]. The uptake activity of the C270A control under reduced Na^+ conditions was 81.55 $\pm$ 4.58 pmol/min/mg protein; this amounts to a sodium activation ratio of 0.78 $\pm$ 0.04, reflecting a moderate sensitivity to changes in [Na^+]. Within TM7, only six mutants (S294C, I295C, F296C, I303C, F304C, and G306C) experienced significant ($p \leq 0.05$) reductions in uptake activity compared with the parental control (Fig. 6). It is noteworthy that mutant F287C displayed a consistent 2-fold increase in Na^+ dependence. At the moment, we are unable to provide a suitable explanation for this unusual result. In general, the native protein couples two molecules of Na^+ to every one bile acid molecule transported with a Hill coefficient of $n = 2$ for Na^+ (Weinman et al., 1998). Because a Hill coefficient >1 may predict positive cooperativity during binding events, we postulate the existence of multiple, distinct binding sites for the pair of Na^+ ions. Because the binding of one Na^+ triggers conformational changes that probably influence binding of the second Na^+ molecule, we can conclude that alterations made at the molecular level along any portion of this transduction pathway (either at binding sites or conformationally involved residues) will modulate subsequent transporter function. From these assumptions, we can hypothesize that 1) these sodium-responsive residues are not directly involved in Na^+ binding because initial mutation to cysteine did not immediately abrogate function and 2) instead, these regions are likely to transduce conformational changes between the two putative

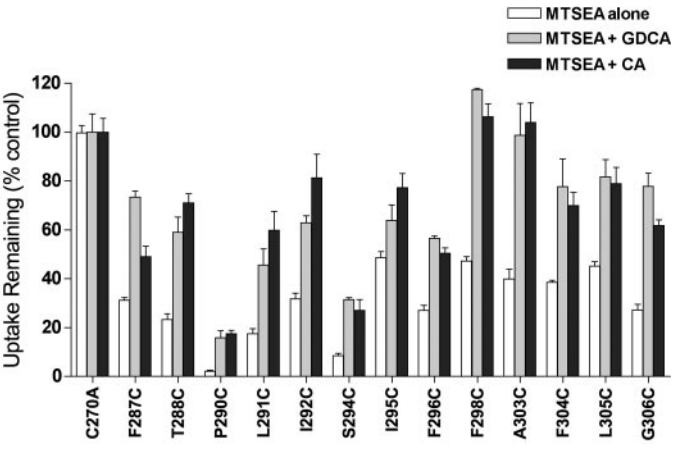

Fig. 5. Effects of bile acid substrates on MTSEA sensitivity for TM7 cysteine double mutants. COS-1 cells transfected with mutants were preincubated with 2.5 mM MTSEA alone or in the presence of GDCA or CA (200 μM) for 10 min at room temperature. Cells were then washed twice and assayed for remaining [^{3}H]taurocholate activity. Control wells without MTSEA were washed and similarly processed. Uptake for each mutant was normalized to its respective control and expressed as a percentage of the C270A parent. Uptake for the C270A mutant in the presence of MTSEA alone was 98.52 $\pm$ 2.86 pmol/min/mg protein, whereas the coincubation with GDCA and CA restored uptake to 118.69 $\pm$ 8.51 and 117.72 $\pm$ 6.36 pmol/min/mg protein, respectively. Bars represent the mean $\pm$ S.D of at least two separate experiments. All mutants were significantly protected by both bile acid substrates ($p <$ 0.05) compared with C270A. For the sake of clarity, asterisks denoting significance have been omitted.

Na^+ binding regions. For mutants I303C, F304C, and G306C, cysteine substitution may have produced molecular alterations that did not apparently alter function at 137 mM [Na^+]; however, conditions of Na^+ paucity combined with these moderate mutational consequences led to severely inhibited (≤30% activity of C270A parent) transport function. The sodium-sensitivity of S294C, I295C, and F296C are especially interesting in lieu of their original increased activities upon cysteine mutation. In particular, the increased transport activity of F296C despite its diminished surface expression (compared with C270A parent) was noted for possibly indicating a decrease in K_m. It is possible that cysteine substitution at these positions created favorable local interactions or enhanced pre-existing ones such that transport activity subsequently increased. With a scarcity of extracellular sodium, activity was acutely reduced compared with original rates of uptake, as reflected by significantly decreased sodium ratios. All six sodium-sensitive mutant transporters were also shown to be highly solvent accessible (Fig. 4), further substantiating their proximity to sites of substrate interaction.

Solvent Accessibility Analysis. Using a previously developed homology model for hASBT (Zhang et al., 2004), the SiteID program within Sybyl was used to probe solvent accessibility of the amino acid residues constituting the inner core of the protein, thereby potentially revealing buried protein domains that could play a key role in substrate and/or cation translocation. Using default settings, the program initially identified 10 solvent pockets, five of which contained fewer than 15 grid points. After filtering redundant clusters, the remaining solvent pockets had molecular volumes of 199,

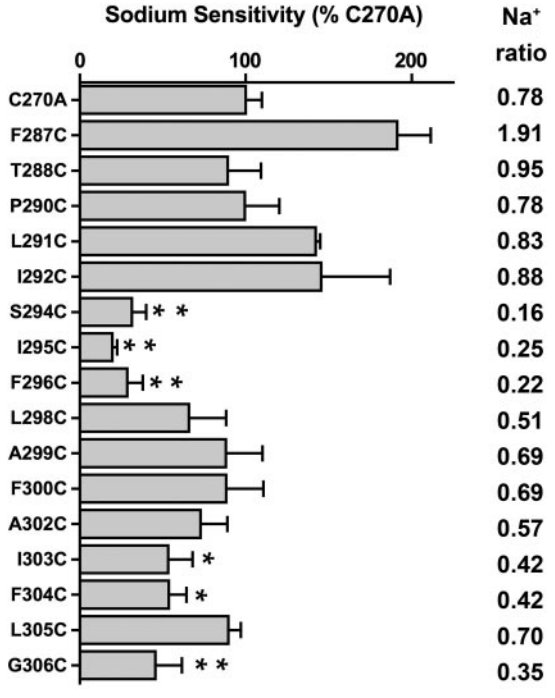

Fig. 6. Sodium activation analysis of functionally active TM7 cysteine mutants. Transfected COS-1 cells were assayed for [^{3}H]taurocholate activity in buffers containing 12 mM [Na^+] and 137 mM [Na^+]. For each mutant, the ratio of uptake at 12 mM versus 137 mM [Na^+] was calculated and expressed as a percentage of C270A control (100%), which has a ratio of 0.78 ± 0.04. Bars represent mean ± S.D. of three separate experiments. **, $p \leq 0.01$; *, $p \leq 0.05$, compared with C270A parent.

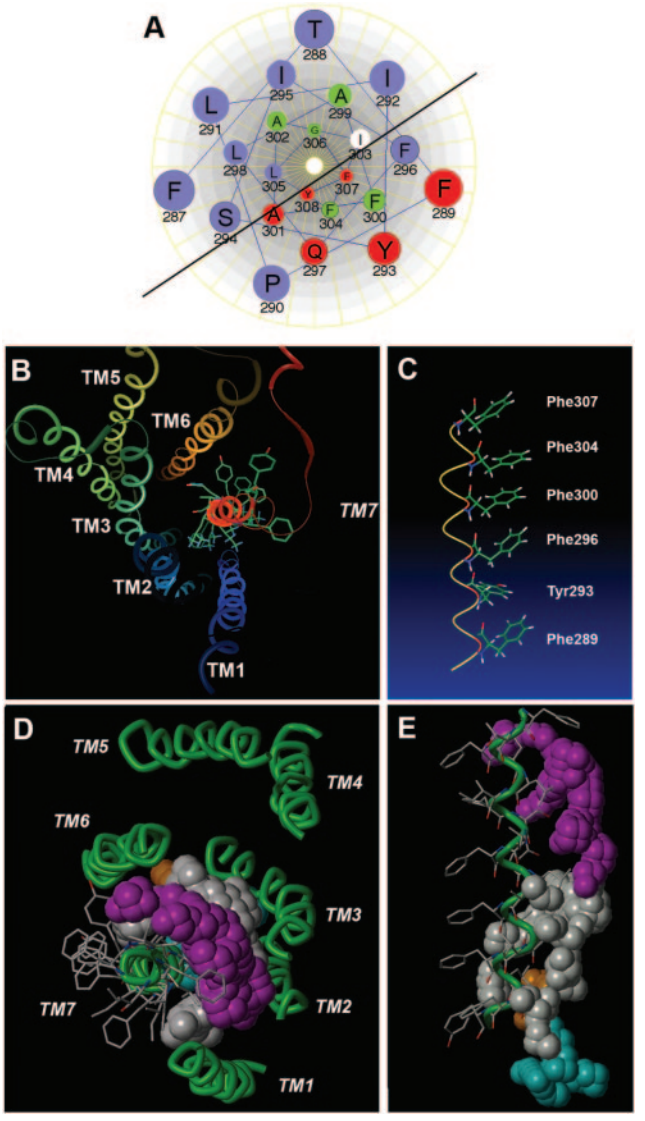

Fig. 7. Computational analysis of hASBT. A, helical wheel representation of TM7 as viewed from the exofacial side of the plasma membrane (Lasergene 6.0; DNAstar, Inc., Madison, WI). Amino acids are represented by their single-letter codes and corresponding placement within the protein. Purple spheres indicate residues that are affected by MTSES and MTSET; red spheres designate loss-of-function residues that are likely to provide a structural anchor within the membrane; residues that are exclusively affected by MTSEA are identified by green spheres; white spheres specify residues that are not significantly ($p > 0.05$) affected by MTS reagents. The solid black line indicates the boundary between residues that constitute functional and structural faces of the TM. B, cytosolic view of the three-dimensional arrangement of hASBT, highlighting the orientation of the transmembrane helices and cytosolic/extracellular regions. Side chains of residues along TM7 have been displayed to visualize the localization of membrane-oriented aromatic amino acids in relation to those residues facing the inner core of the protein. For clarity, hydrogen atoms were omitted, and depth cueing was set to emphasize the transmembrane domains. C, predicted three-dimensional α-helical arrangement of functionally hampered cysteine mutants along vertical axis of TM7. D, solvent accessibility analysis of hASBT. The grid method within SiteID was used to determine accessible regions of a previously developed homology model of the hASBT protein (Zhang et al., 2004). Major clusters are visualized by colored spheres. For clarity, only clusters surrounding TM7 were visualized; accordingly, cluster 5 (44 Å^3) was omitted. The resulting gray, yellow, cyan, and magenta clusters (2, 3, 4, and 6) have molecular volumes of 199, 57, 29, and 90 Å^3, respectively, and occupy domains spatially favorable to the formation of hydrogen bonds with TM7 amino acids Phe287, Pro290, Leu298, Ala301, Ala302, and Leu305. E, side view of the solvent-accessible pockets surrounding TM7 as described in D.

57, 110, 44, and 90 Å^3 (defined as clusters 2–6, respectively) (Fig. 7, D and E). It is noteworthy that four of the five main solvent pockets are directly adjacent to TM7 (clusters 2, 3, 4, and 6; visualized as gray, yellow, cyan, and magenta, respectively) and predominantly line the hydrophilic face of this transmembrane domain (Figs. 7, D and E), suggestive of a highly accessible pathway. Based on these data, it can be deduced that TM7, in conjunction with other TMs, plays a dominant role in the translocation process.

Discussion

This study examined the functional consequences of individual cysteine substitution of 22 amino acids comprising TM7 of hASBT followed by evaluation of its accessibility to MTS derivatives. An MTS-resistant mutant, C270A, provided the background for introduction of subsequent cysteine mutations, thereby circumventing the thiol-sensitivity of native hABST and inability to generate a Cys-less transporter typically required for SCAM analysis. Although this general protocol has been extended to various polytopic proteins (Frillingos et al., 1998), the current study represents the first application of SCAM to the SLC10 family.

Our results clearly demonstrate the marked solvent accessibility of TM7, consisting of residues Phe288 to Tyr308, and the significance of TM7 to hASBT transport activity, in general. We propose two distinct roles for TM7 amino acids, encompassing both structural and functional consequences to transporter activity and specifically, modulating interactions with substrates during translocation. We posit that six amino acids lining one face of TM7 (Phe289, Tyr293, Gln297, Ala301, Phe307, and Tyr308) comprise a structural anchor within the TM necessary for transporter activity (Fig. 7C). Highly aqueous-accessible amino acids are contained along TM faces mainly adjacent to and opposite this structural region (Fig. 7A), forming interfaces for substrate interaction accessible from the extracellular matrix. Structural and functional roles for TM7 are based on the following observations: 1) MTS probing of the water-accessible surface of TM7 demonstrated a high degree of accessibility to hydrophilic, charged MTS reagents; 2) hydrophilic, charged bile acid substrates, GDCA and CA, conferred significant protection against thiol modification to all MTSEA-sensitive cysteine mutants; 3) upon initial mutation to cysteine, severe loss of activity was observed for amino acids Phe289, Tyr293, Gln297, and Ala301, demonstrating an α-helical periodicity of four along this region; 4) it seems unlikely that a highly water-accessible pathway would exist through an essential membrane spanning domain if it did not participate in substrate translocation, especially in a relatively small protein. As demonstrated by computational analysis, water-accessible regions are present along other TM regions (Fig. 7); however, they putatively work in combination with TM7 to form a pore or channel directing ligand movement through the membrane.

Because cysteine replacement of six TM7 amino acids resulted in complete loss of function (Q297C, F307C, Y308C) or severely depressed activity ($\leq$20% activity) (F289C, Y293C, A301C), we conclude that these sites cannot tolerate cysteine substitution. Furthermore, Phe289, Tyr293, Gln297, and Ala301 are positioned as every fourth residue, forming a pattern clearly suggestive of an α-helix along the exofacial segment of TM7 (Fig. 6, A and C). Moreover, residues with measurable residual activity (Phe289, Tyr293, and Ala301) were not MTS-sensitive. We can therefore assign structural roles to these six residues that are necessary in maintaining specific configurations of TM7 that are disrupted upon cysteine substitution. Because replacement with sulfhydryl side chains constitutes a nonconservative mutation for these amino acids, we can speculate that function may be abrogated either through unfavorable local interactions with adjacent amino acids or large-scale disruption of protein conformations vital for activity. Finally, Phe307 emerges as especially important in proper folding and stability of the translated protein, as suggested by its lack of expression upon cysteine substitution. Likewise, the severe loss of activity for Y308C coupled with its reduced membrane expression strongly implies the structural bearings of this residue in transporter function.

Apart from its structural role, we propose that TM7 is highly accessible from the extracellular matrix for solvent-based interactions (Fig. 4). Helical wheel projection of TM7 (Fig. 6A) reveals that residues accessible to membrane-impermeant MTS reagents constitute regions separate from the proposed structural elements of the TM. Because the oppositely charged MTSES and MTSET produced similar inhibition profiles along the extracellular half of the TM, we postulate that modification is independent of electrostatic effects. Although not statistically significant, MTSES moderately inhibited a number of residues within the cytosolic half of TM7, suggesting that variability in thiol modification may correlate to differences in molecular volume. This hypothesis is strengthened by the enhanced accessibility of the cytosolic region to the relatively smaller MTSEA. Thus, we posit that a size restriction exists along the TM that is proportional to the molecular volume of the MTS derivative applied. Correspondingly, MTSEA may circumvent this barrier either through its decreased bulk, slight membrane permeability or enhanced concentrations (2.5 mM). Our model of TM7 accessibility is further corroborated by the computationally derived solvent-accessible pockets that demonstrate a concomitant decrease in accessible molecular volume traveling deeper into the membrane toward the cytosolic interface of the TM (Fig. 6C). Thus, we conclude that the solvent accessibility of TM7 predicts its involvement in substrate translocation.

Furthermore, the results of bile acid protection studies complement the proposed interaction of TM7 with natural hASBT substrates. The majority of thiol-sensitive mutant transporters experienced significant ($p \leq 0.05$) restoration of activity upon coincubation of bile acid substrates (GDCA, CA) with MTSEA. Although additional studies are needed to unequivocally demonstrate the precise origin of substrate protection, our data suggest that the decidedly significant blockage of MTSEA modification is a result of the physical presence of bile acids within the highly solvent accessible regions of TM7.

Because hASBT requires the presence of Na^+ to energize active bile acid transport, the influence of this cotransported ion on mutant activity was investigated. Our data suggest that TM7 residues may transduce conformational changes associated with binding of the two sodium molecules at their respective binding sites (Fig. 6). We infer this indirect role in sodium interaction because the functional consequences of

cysteine mutation were only apparent at low (12 mM) [Na^+] for the six sodium-sensitive sites (S294C, I295C, F296C, Ile303, Phe304, G306C). Therefore, direct involvement in Na^+ binding is unlikely for this region.

Finally, the congenital P290S mutation implicated in primary bile acid malabsorption (Wong et al., 1995) is localized to TM7. Although a Pro→Ser conversion at this position would suggest direct involvement of this residue in bile acid interaction, the mutant transporter P290C retained activity (Fig. 3D), although it was highly susceptible to MTS modification (Fig. 4). Proline residues play important structural and functional roles in transporters. They can form conformational switches in TM α-helices that enable the changes critical for substrate translocation (Sansom, 1992; Paczkowski and Bryan-Lluka, 2004). Because initial mutation of Pro290 did not significantly decrease transport activity, we can conclude that the presence of proline at this position is not strictly required. Although MTS accessibility indicated a highly water-accessible site at this residue, the lack of complete restoration of activity by bile acid protection further negates the possibility of direct ligand binding at this position. It is noteworthy that P290C is juxtaposed by two loss-of-function sites (Fig. 6A), implicated in maintaining the structural integrity of the α-helix in TM7 (Gln297, Ala301). Therefore, we conclude that Pro290 does not directly interact with substrate but is likely to play a structural role in TM7 by transducing conformational changes associated with ligand translocation.

In summary, the implications of the present study strengthen the previously suggested role of TM7 in hASBT transport activity. In particular, our findings assign a direct role to TM7 in substrate translocation using an investigational protocol (SCAM) uniquely applied to a previously unscrutinized region of hASBT. Although the process of substrate translocation for any given membrane-bound transporter is obviously complex and may involve many of its regions, the implications of this study provide novel evidence for the involvement of a conserved membrane segment during the internalization process.

References

Akabas MH, Stauffer DA, Xu M, and Karlin A (1992) Acetylcholine receptor channel structure probed in cysteine-substitution mutants. *Science (Wash DC)* **258:**307–310.

Alrefai WA, Sarwar Z, Tyagi S, Saksena S, Dudeja PK, and Gill RK (2005) Cholesterol modulates human intestinal sodium-dependent bile acid transporter. *Am J Physiol* **288:**G978–G985.

Banerjee A, Ray A, Chang C, and Swaan PW (2005) Site-directed mutagenesis and use of bile acid-MTS conjugates to probe the role of cysteines in the human apical sodium-dependent bile acid transporter (SLC10A2). *Biochemistry* **44:**8908–8917.

Banerjee A and Swaan PW (2006) Membrane Topology of Human ASBT (SLC10A2) Determined by dual label epitope insertion scanning mutagenesis. New evidence for seven transmembrane domains. *Biochemistry* **45:**943–953.

Chen JG, Liu-Chen S, and Rudnick G (1997) External cysteine residues in the serotonin transporter. *Biochemistry* **36:**1479–1486.

Chiang JY, Kimmel R, and Stroup D (2001) Regulation of cholesterol 7alpha-hydroxylase gene (CYP7A1) transcription by the liver orphan receptor (LXRalpha). *Gene* **262:**257–265.

Craddock AL, Love MW, Daniel RW, Kirby LC, Walters HC, Wong MH, and Dawson PA (1998) Expression and transport properties of the human ileal and renal sodium-dependent bile acid transporter. *Am J Physiol* **274:**G157–G169.

Frillingos S, Sahin-Toth M, Wu J, and Kaback HR (1998) Cys-scanning mutagenesis: a novel approach to structure function relationships in polytopic membrane proteins. *FASEB J* **12:**1281–1299.

Geyer J, Godoy JR, and Petzinger E (2004) Identification of a sodium-dependent organic anion transporter from rat adrenal gland. *Biochem Biophys Res Commun* **316:**300–306.

Geyer J, Wilke T, and Petzinger E (2006) The solute carrier family SLC10: more than a family of bile acid transporters regarding function and phylogenetic relationships. *Naunyn-Schmiedeberg's Arch Pharmacol* **372:**413–431.

Hallén S, Bjorquist A, Ostlund-Lindqvist AM, and Sachs G (2002) Identification of a region of the ileal-type sodium/bile acid cotransporter interacting with a competitive bile acid transport inhibitor. *Biochemistry* **41:**14916–14924.

Hallén S, Fryklund J, and Sachs G (2000) Inhibition of the human sodium/ bile acid cotransporters by side specific methanethiosulfonate sulfhydryl reagents: substrate controlled accessibility of site of activation. *Biochemistry* **39:**6743–6750.

Holmgren M, Liu Y, Xu Y, and Yellen G (1996) On the use of thiol-modifying agents to determine channel topology. *Neuropharmacology* **35:**797–804.

Huff MW, Telford DE, Edwards JY, Burnett JR, Barrett PH, Rapp SR, Napawan N, and Keller BT (2002) Inhibition of the apical sodium-dependent bile acid transporter reduces LDL cholesterol and apoB by enhanced plasma clearance of LDL apoB. *Arterioscler Thromb Vasc Biol* **22:**1884–1891.

Izzat NN, Deshazer ME, and Loose-Mitchell DS (2000) New molecular targets for cholesterol-lowering therapy. *J Pharmacol Exp Ther* **293:**315–320.

Javitch JA (1998) Probing structure of neurotransmitter transporters by substituted-cysteine accessibility method. *Methods Enzymol* **296:**331–346.

Karlin A and Akabas MH (1998) Substituted-cysteine accessibility method. *Methods Enzymol* **293:**123–145.

Kramer W, Girbig F, Glombik H, Corsiero D, Stengelin S, and Weyland C (2001) Identification of a ligand binding site in the Na^+/bile acid cotransporting protein from rabbit. *J Biol Chem* **276:**36020–36027.

Kramer W, Stengelin S, Baringhaus KH, Enhsen A, Heuer H, Becker W, Corsiero D, Girbig F, Noll R, and Weyland C (1999) Substrate specificity of the ileal and the hepatic Na^+/bile acid cotransporters of the rabbit. I. Transport studies with membrane vesicles and cell lines expressing the cloned transporters. *J Lipid Res* **40:**1604–1617.

Kulkarni AA, Haworth IS, and Lee VH (2003a) Transmembrane segment 5 of the dipeptide transporter hPepT1 forms a part of the substrate translocation pathway. *Biochem Biophys Res Commun* **306:**177–185.

Kulkarni AA, Haworth IS, Uchiyama T, and Lee VH (2003b) Analysis of transmembrane segment 7 of the dipeptide transporter hPepT1 by cysteine-scanning mutagenesis. *J Biol Chem* **278:**51833–51840.

Li H, Xu G, Shang Q, Pan L, Shefer S, Batta AK, Bollineni J, Tint GS, Keller BT, and Salen G (2004) Inhibition of ileal bile acid transport lowers plasma cholesterol levels by inactivating hepatic farnesoid X receptor and stimulating cholesterol 7 alpha-hydroxylase. *Metabolism* **53:**927–932.

Mitchell SM, Lee E, Garcia ML, and Stephan MM (2004) Structure and function of extracellular loop 4 of the serotonin transporter as revealed by cysteine-scanning mutagenesis. *J Biol Chem* **279:**24089–24099.

Paczkowski FA and Bryan-Lluka LJ (2004) Role of proline residues in the expression and function of the human noradrenaline transporter. *J Neurochem* **88:**203–211.

Root C, Smith CD, Winegar DA, Brieaddy LE, and Lewis MC (1995) Inhibition of ileal sodium-dependent bile acid transport by 2164U90. *J Lipid Res* **36:**1106–1115.

Sansom MS (1992) Proline residues in transmembrane helices of channel and transport proteins: a molecular modelling study. *Protein Eng* **5:**53–60.

Telford DE, Edwards JY, Lipson SM, Sutherland B, Barrett PH, Burnett JR, Krul ES, Keller BT, and Huff MW (2003) Inhibition of both the apical sodium-dependent bile acid transporter and HMG-CoA reductase markedly enhances the clearance of LDL apoB. *J Lipid Res* **44:**943–952.

Trauner M and Boyer JL (2003) Bile salt transporters: molecular characterization, function, and regulation. *Physiol Rev* **83:**633–671.

Weinman SA, Carruth MW, and Dawson PA (1998) Bile acid uptake via the human apical sodium-bile acid cotransporter is electrogenic. *J Biol Chem* **273:**34691–34695.

West KL, Ramjiganesh T, Roy S, Keller BT, and Fernandez ML (2002) 1-[4-[4[(4*R*,5*R*)-3,3-Dibutyl-7-(dimethylamino)-2,3,4,5-tetrahydro-4-hydroxy −1,1-dioxido-1-benzothiepin-5-yl]phenoxy]butyl]-4-aza-1-azoniabicyclo[2.2. 2]octane methanesulfonate (SC-435), an ileal apical sodium-codependent bile acid transporter inhibitor alters hepatic cholesterol metabolism and lowers plasma low-density lipoprotein-cholesterol concentrations in guinea pigs. *J Pharmacol Exp Ther* **303:**293–299.

Wong MH, Oelkers P, and Dawson PA (1995) Identification of a mutation in the ileal sodium-dependent bile acid transporter gene that abolishes transport activity. *J Biol Chem* **270:**27228–27234.

Zhang EY, Phelps MA, Banerjee A, Khantwal CM, Chang C, Helsper F, and Swaan PW (2004) Topology scanning and putative three-dimensional structure of the extracellular binding domains of the apical sodium-dependent bile acid transporter (SLC10A2). *Biochemistry* **43:**11380–11392.

Address correspondence to: Peter W Swaan. Ph.D, University of Maryland, HSF-II, 20 Penn Street, Baltimore, MD 21201. E-mail: pswaan@rx.umaryland.edu